European Review for Medical and Pharmacological Sciences 2022; 26: 6176-6186

A nomogram integrating ferroptosis- and immune-related biomarker for prediction of prognosis and diagnosis in kidney renal clear cell carcinoma

X.-L. XING[1,2], Y. LIU[1], J.-H. LIU[1], H.-F. ZHOU[1], H.-R. ZHANG[1], Q. ZUO[3], P. BU[1], T. DUAN[3], Y. ZHOU[3], Z.-Q. XIAO[1]

[1]Changsha Central Hospital, University of South China, Changsha, China
[2]School of Public Health and Laboratory Medicine, Hunan University of Medicine, Huaihua, China
[3]First Hospital of Changsha, Changsha, China

Abstract. – OBJECTIVE: Approximately 60% of patients with kidney renal clear cell carcinoma (KIRC) die within the first 2-3 years. The prognosis for patients with KIRC and its metastases is poor. Ferroptosis and providing immunity are novel treatment targets for several cancers, including KIRC. Therefore, it is important to identify suitable ferroptosis- and immune-related signatures to predict the prognosis and diagnosis of patients with KIRC.

MATERIALS AND METHODS: The corresponding data of patients with KIRC were obtained from the Cancer Genome Atlas. Univariate and multivariate Cox regression analyses were used to screen candidate biomarkers in patients with KIRC.

RESULTS: We found that four FI-DEGs (BID, MET, LTB4R, and HMOX1) were independently associated with the overall survival of patients with KIRC. The prognosis and diagnosis model constructed using these four biomarkers could predict the outcome of KIRC, as measured by the receiver operating characteristic analyses.

CONCLUSIONS: We identified 4 FI-DEGs that could be used as biomarkers in patients with KIRC. The present study not only contributes to understanding the roles of ferroptosis and immunity in the development of KIRC, but also to the diagnosis and prognosis of KIRC, although it remains to be further studied.

Key Words:
KIRC, Ferroptosis, Immune, Prognosis, Diagnosis.

Introduction

The latest edition of global cancer statistics shows that kidney cancer is the sixteenth most common cancer[1]. In 2020, there were more than 400,000 new cases (2.2%) and approximately 180,000 cases of kidney cancer. Kidney renal clear cell carcinoma (KIRC) is a malignant cancer originating from the renal epithelium that accounts for approximately 75% of kidney cancer cases[2]. Although the overall 5-year survival rate of KIRC is approximately 75%, treatment of patients with advanced and metastatic KIRC remains a significant challenge because of its resistance to chemotherapy and radiation therapy[3]. Moreover, more than 30% of patients with KIRC develop metastasis[4]. The 5-year survival rate of patients with metastasis is lower than 10%, and the median survival is only 13 months[5]. Early diagnosis failure and drug resistance are widely believed to be the main reasons for the poor prognosis of patients with metastatic KIRC. Therefore, the development of new drugs and identification of new biomarkers play important roles in the treatment and prognosis of KIRC[6].

Recent evidence[7,8] indicates that multiple targeted therapies have improved the long-term survival of advanced-stage KIRC. Regulation of ferroptosis and immunity are novel therapeutic targets for treating cancer that have been discovered in recent years. Moreover, a large amount of evidence has shown that ferroptosis can regulate anticancer immunity by interacting with immune cells, such as NK cells and CD8+ T cells[9-11]. Ferroptosis attenuates antitumor immunity by affecting cDC1s and NK cells[12]. Previous studies[13,14] have also shown that ferroptosis and the immune system may have synergistic effects with respect to cancer treatment. Therefore, in the present study, we conducted an integrated analysis of ferroptosis- and immune-related genes to explore their

Corresponding Authors: Y. Zhou, MD; e-mail: 921lan@sina.com
Z.-Q. Xiao, MD; e-mail: xzq1892000@163.com

pathogenesis and to identify potential biomarkers for tumorigenesis, diagnosis, and prognosis.

Materials and Methods

Patients Data Acquisition and Differential Expression Analyses

The count data of RNA_sequencing (RNA_seq) and corresponding clinical information of 530 patients with KIRC and 72 controls were downloaded from the TCGA database (available at: https://portal.gdc.cancer.gov/repository).

The DESeq2 R package was used to screen the differentially expressed genes (DEGs) between the controls and patients with KIRC, as well as between patients with KIRC with a high-risk value and those with a low-risk value. The criteria were set as follows: mean ≥ 500, $|\log FoldChange| \geq 1$, and p adj < 0.05.

Identification of Ferroptosis- and Immune-related DEGs

The recognized ferroptosis- and immune-related (FI) genes were downloaded from the FerrDb (available at: http://www.zhounan.org/ferrdb) and ImmPort (available at: http://www.immport.org) databases, respectively. Overlapping analyses were performed on DEGs and FI-genes to identify differentially expressed ferroptosis- and immune-related genes (FI-DEGs).

Construction and Validation of a Prognosis Model

Patients with KIRC were divided into low- and high-expression cohorts, according to the median expression value of each FI-DEG. Univariate Cox regression analyses were used to evaluate the relationship of the FI-DEGs with the overall survival of KIRC patients, followed by least absolute shrinkage and selection operator (LASSO) regression analyses. Multivariate Cox regression analysis was used to screen for candidate biomarkers.

According to a previous method, candidate biomarkers were used to evaluate the risk value of each patient. Risk score=, where n represents the gene number, Coei represents the coefficient value, and Expi represents the gene expression level[15]. We developed a comprehensive index of ferroptosis and immune status (CIFI) using the risk values. CIFI = (risk score - min)/Max[15]. The Youden index was used as an optimal cut-off value to regroup patients with KIRC.

Construction and Validation of a Diagnosis Model

A diagnostic model integrating candidate biomarkers was established to distinguish KIRC from normal subjects using a stepwise logistic regression method. Diagnostic scores were identified as follows: LOGIT = 0.551 + (0.205 × LTB4R expression level) + (0.166 × MET expression level) + (0.155 × HMOX1 expression level) + (0.133 × BID expression level)[15].

Estimation of Tumor-Infiltrating Immune Cells

The proportion of different tumor-infiltrating immune cells and factors were downloaded from the Tumor IMmune Estimation Resource (available at: https://cistrome.shinyapps.io/timer/). Pearson correlation analyses were used to evaluate the relationship between ESTIMATE, immune cells, immune factors, and the CIFI value.

Functional Enrichment and Interaction analyses

The Database for Annotation, Visualization and Integrated Discovery (DAVID, v. 6.8) was used to perform Gene Ontology (GO) and Kyoto Encyclopedia of Genes and Genomes (KEGG) pathway enrichment analyses using the default parameters. STRING (11) was used to assess protein-protein interactions using the default parameters, and Cytoscape (3.7.2) was used to visualize protein-protein interactions.

Statistical Analysis

An unpaired two-tailed Student's t-test was used, as indicated. All results were expressed as mean ± SEM.

Results

Identification of FI-DEGs as Prognosis Biomarkers

A total of 2,336 DEGs (1,455 DEGs were upregulated and 881 DEGs were downregulated) were identified by analyzing the RNA_seq count data of patients with KIRC. Out of which, 545 FI-DEGs (62 ferroptosis-related DEGs and 483 immune-related DEGs) were identified by overlapping analysis (Figure 1a). Univariate Cox regression analyses revealed that 96 FI-DEGs were associated with OS in KIRC (Figure 1b). The interactions between these 96 FI-DEGs are shown in Figure 1c. To avoid over-fitting, we introduced

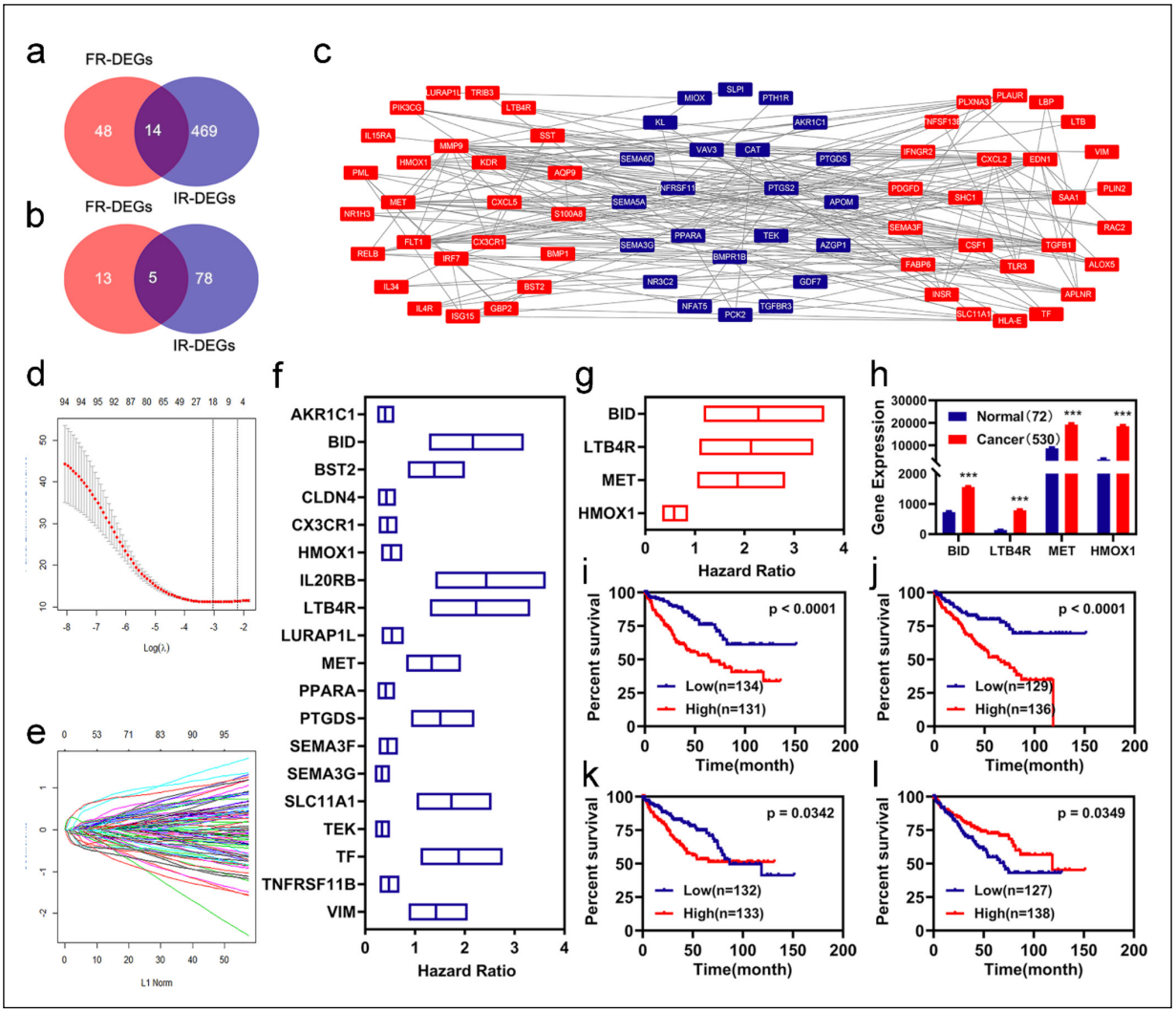

Figure 1. Identification of FI-DEGs as Prognosis Biomarkers. **a**, Approximately, 545 FI-DEGs were identified by overlapping analyses. **b**, Univariate Cox regression analyses identified 96 FI-DEGs associated with the OS of KIRC. **c**, The protein interactions of those 96 FI-DEGs. **d-e**, Over-fitting analyses for those 96 FI-DEGs. **f**, 19 FI-DEGs were identified to be associated with the OS of KIRC by univariate Cox regression analyses. **g**, Four FI-DEGs were identified to be associated with the OS of KIRC by multivariate Cox regression analyses. **h**, The expression status of the four FI-DEGs between the controls and KIRC patients. **i-l**, Overall survival curve of those four FI-DEGs in the training cohort. * $p < 0.05$, ** $p < 0.01$, *** $p < 0.001$.

LASSO analyses for the 96 FI-DEGs (Figure 1d-1e) and found that 19 FI-DEGs were still associated with the OS of KIRC (Figure 1f).

To obtain and verify suitable biomarkers, we first randomly divided the patients into two cohorts (training and validation cohorts). Subsequently, multivariate Cox regression analyses were performed for the 19 FI-DEGs in the training cohort, and we found that four FI-DEGs were independently associated with the OS of patients with KIRC (Figure 1g). The expression of these four FI-DEGs was markedly increased in patients with KIRC (Figure 1h). Patients with low expression of BID, MET, and LTB4R displayed better OS, whereas patients with low expression of HMOX1 displayed worse OS (Figure 1i-1l).

Construction and Validation of the Prognosis Model

Based on previous studies, we constructed a CIFI risk assessment model using four FI-DEGs in the training cohort. The CIFI value (top) and survival status (bottom) of each patient with KIRC are shown in Figure 2a. Patients with KIRC and high CIFI values displayed worse OS (Figure 2b). Receiver operating characteristic curve

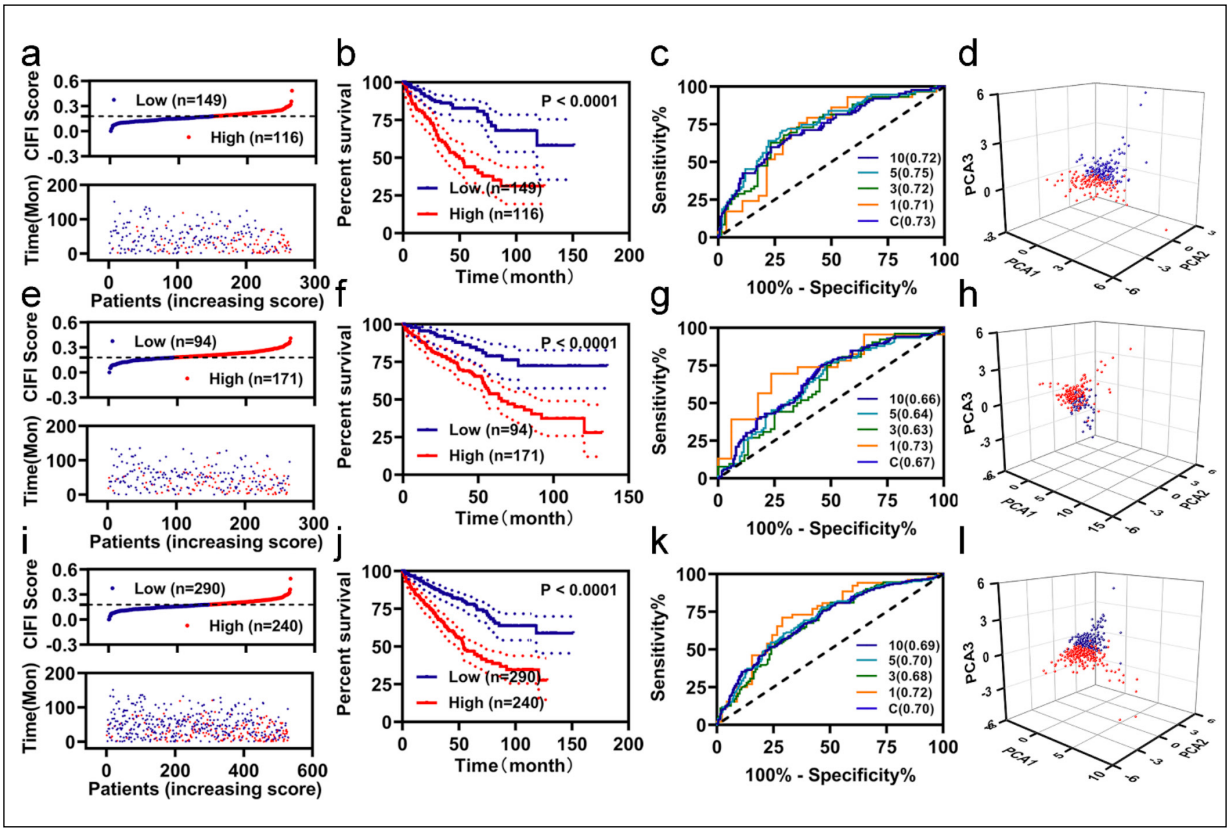

Figure 2. Construction and validation of CIFI as prognosis model. **a**, **e**, and **i**, CIFI value (up) and survival status (down) for each patient in the training cohort (**a**), validation cohort (**e**), and entire cohort (**i**). **b**, **f**, and **j**, Overall survival curve of patients with KIRC with different CIFI value in the training cohort (**b**), validation cohort (**f**), and entire cohort (**j**). **c**, **g**, and **k**, ROC curve of risk assessment model in the training cohort (**c**), validation cohort (**g**), and entire cohort (**k**). **d**, **h**, and **l**, Distribution of patients with different CIFI value in the training cohort (**d**), validation cohort (**h**), and entire cohort (**l**) by PCA analyses. Red indicates the patients with KIRC with high CIFI risk value. Blue indicates the patients with KIRC with low CIFI risk value.

(ROC) analysis indicated that the area under the ROC curve (AUC) reached 0.73 (Figure 2c). Additionally, we performed a time-dependent ROC curve analysis. The AUC values of the prognostic model in the training cohort reached 0.71, 0.72, 0.75, and 0.72 at 1, 3, 5, and 10 years, respectively (Figure 2c). Principal component analysis showed that the patients with KIRC with high-risk values could be well distinguished from those with low-risk values (Figure 2d).

To determine whether the model was feasible, we performed similar analyses in both the validation cohort and the entire cohort. Similar results are shown in Figure 2e-2l. In particular, we found that the AUC values of the CIFI risk model in the validation cohort and entire cohort were 0.67 and 0.70, respectively (Figure 2g and 2k). Patients with KIRC with low-risk values could be distinguished from those with high-risk values (Figure 2h, 2l).

Independent Prognostic Evaluation of the Prognosis Model

To determine whether the CIFI risk model and different clinical characteristics, including pathologic TNM, pathologic stage, age, and sex, can be used as independent diagnostic factors, we performed univariate and multivariate Cox regression analyses for those signatures in the entire cohort. In the CIFI risk model, age and pathologic NM were independently associated with the OS of patients with KIRC (Figure 3a-3b). ROC analyses were then performed for the CIFI risk model and to determine the clinical characteristics. Although in the CIFI risk model, pathologic NM, and age were independently associated with the OS of KIRC patients, the AUC value of the CIFI risk model was higher than that of the pathologic NM and age (Figure 3c).

Moreover, we investigated the expression status of these four FI-DEGs between patients with KIRC with high and low CIFI risk values. The expression

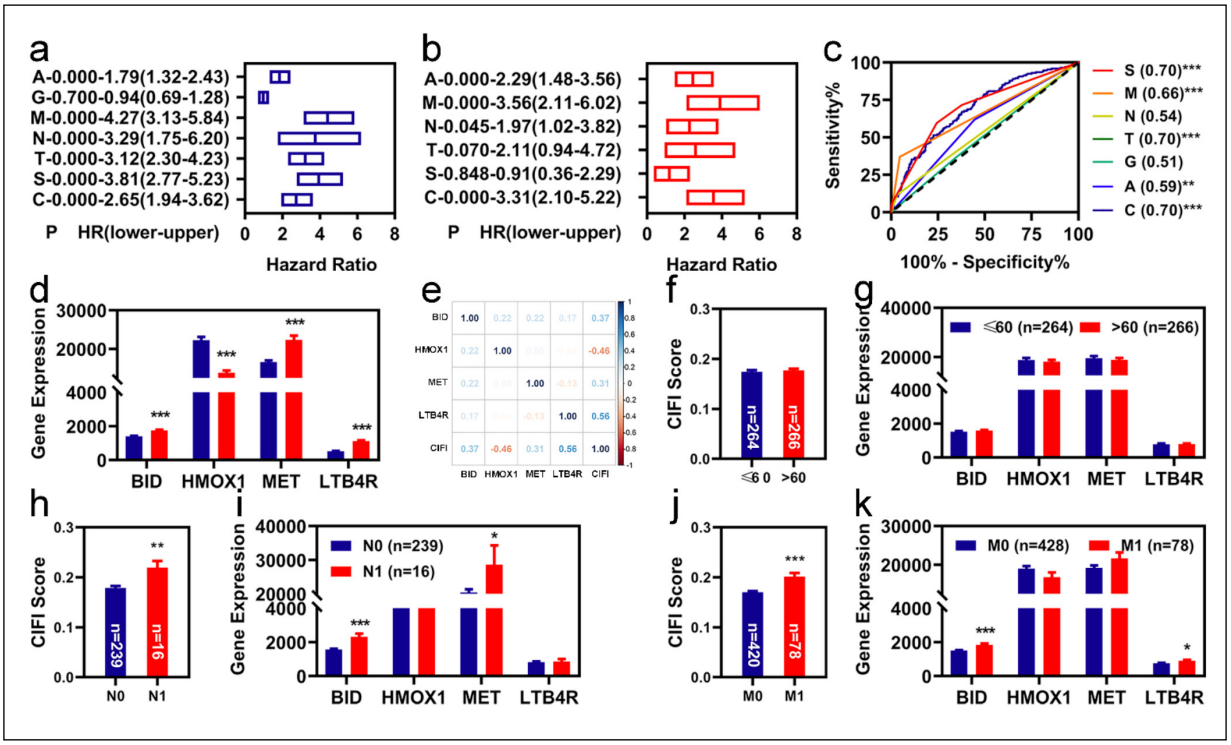

Figure 3. Independent prognostic values of the 4 FI-DEGs. **a**, Univariate Cox regression analyses illustrated six clinical characteristics and CIFI value were correlated with OS of patients with KIRC. **b**, Multivariate Cox regression analyses illustrated three clinical characteristics and CIFI value were correlated with the OS of patients with KIRC independently. **c**, ROC curve of different clinical characteristics and CIFI value. **d**, The expression status of those four prognostic biomarkers in the groups with different CIFI value. **e**, Correlation of the four FI-DEGs with the CIFI value. **f-k**, CIFI score and expression of four FI-DEGs within different clinical characteristics. * $p < 0.05$, ** $p < 0.01$, *** $p < 0.001$.

of BID, MET, and LTB4R considerably increased, whereas the expression of HMOX1 markedly decreased in patients with KIRC with high CIFI risk values (Figure 3d). Correlation analyses indicated that the CIFI value was positively correlated with BID, MET, and LTB4R, and negatively correlated with HMOX1 (Figure 3e).

Since pathologic NM, age, and the CIFI risk model were independently associated with the OS of KIRC, we also analyzed the expression of these four FI-DEGs and CIFI values in different age and NM groups. The results are shown in Figures 3f-3k.

The Immune Cell Infiltration Landscape in KIRC

To determine the relationship between the CIFI risk model and immunity, we first performed ESTIMATE analyses for the controls and patients with KIRC and found that the estimated score, stromal score, and immune score markedly increased in the KIRC patients (Figure 4a-4c). Moreover, the tumor purity score markedly decreased in patients with KIRC (Figure 4d). Correlation analyses showed that the CIFI value was not correlated with the four ESTIMATE scores (Figure 4e) but was markedly correlated with several immune cells (Figure 4f).

We also performed similar analyses for the KIRC patients with different CIFI risk values. The estimated score, stromal score, and tumor purity markedly increased in patients with KIRC with high CIFI values (Figure 4g-4i). There was no significant difference between the patients with different CIFI risk scores (Figure 4j). Moreover, correlation analyses also showed that the CIFI value was not correlated with the four ESTIMATE scores (Figure 4k) but was markedly correlated with several immune cells (Figure 4l).

Immune-Related Pathways Were Enriched in the High CIFI Risk Group

To further determine whether there was a difference in immunity between patients with KIRC and different CIFI risks, we carried out differential expression analyses and found that there were 132 DEGs (116 upregulated DEGs and 16 down-

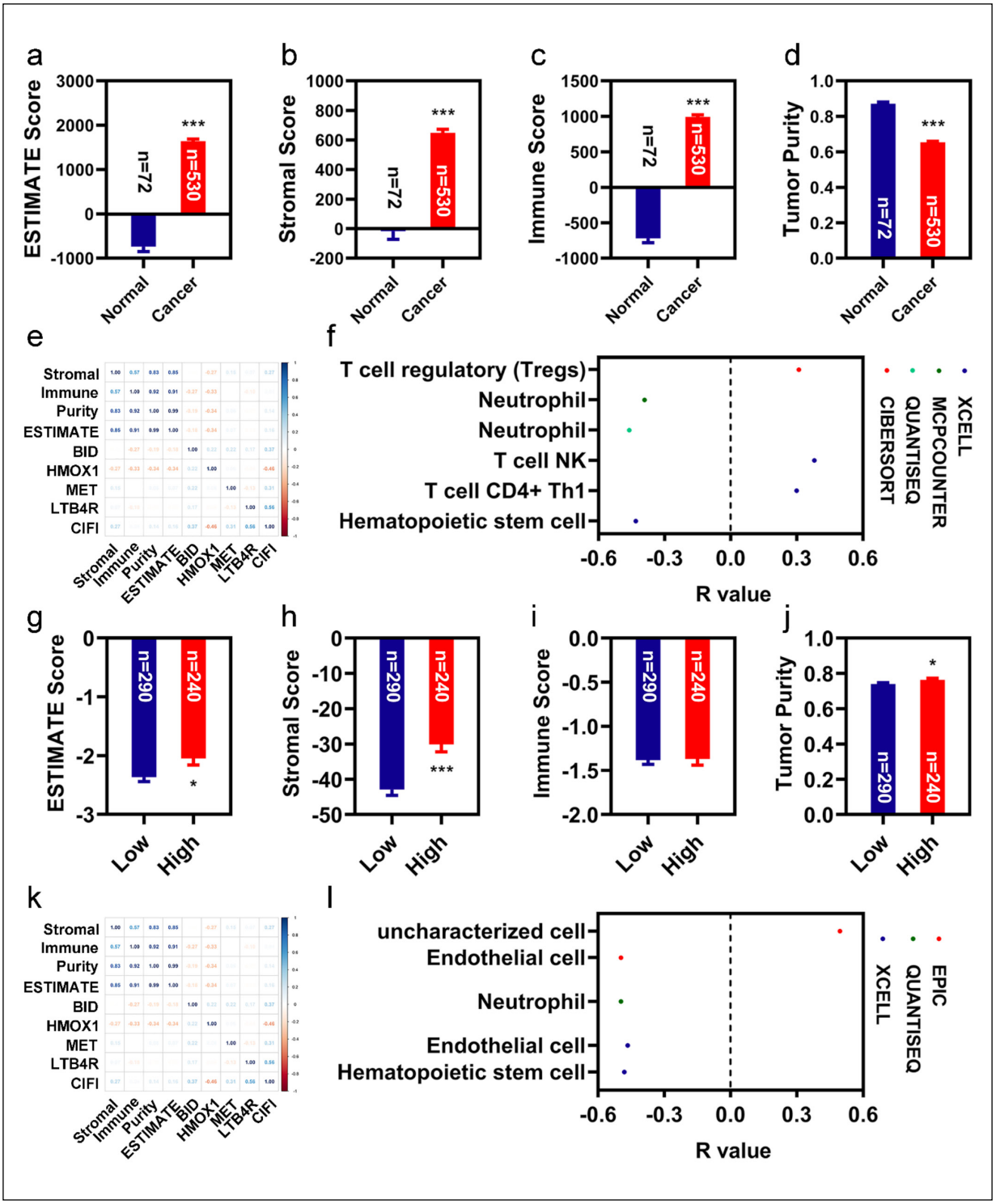

Figure 4. Correlation analyses of CIFI with immunity. ***a-d***, Immune score between normal and patients with KIRC in all samples (controls and KIRC patients). **a**, estimate score. **b**, stromal score. **c**, immune purity. **d**, tumor purity. **e**, Correlation analyses of ESTIMATE score with the four prognostic biomarkers in all samples (controls and KIRC patients). **f**, Correlation analyses of CIFI value with the immune cells in all samples (controls and KIRC patients). ***g-j***, Immune score between control and patients with KIRC in all samples (controls and KIRC patients). **g**, estimate score. **h**, stromal score. **i**, immune purity. **j**, tumor purity. **k**, Correlation analyses of ESTIMATE score with the four prognostic biomarkers in patients with different CIFI value (low CIFI and high CIFI). **l**, Correlation analyses of CIFI value with the immune cells in patients with different CIFI value (low CIFI and high CIFI). * $p < 0.05$, ** $p < 0.01$, *** $p < 0.001$.

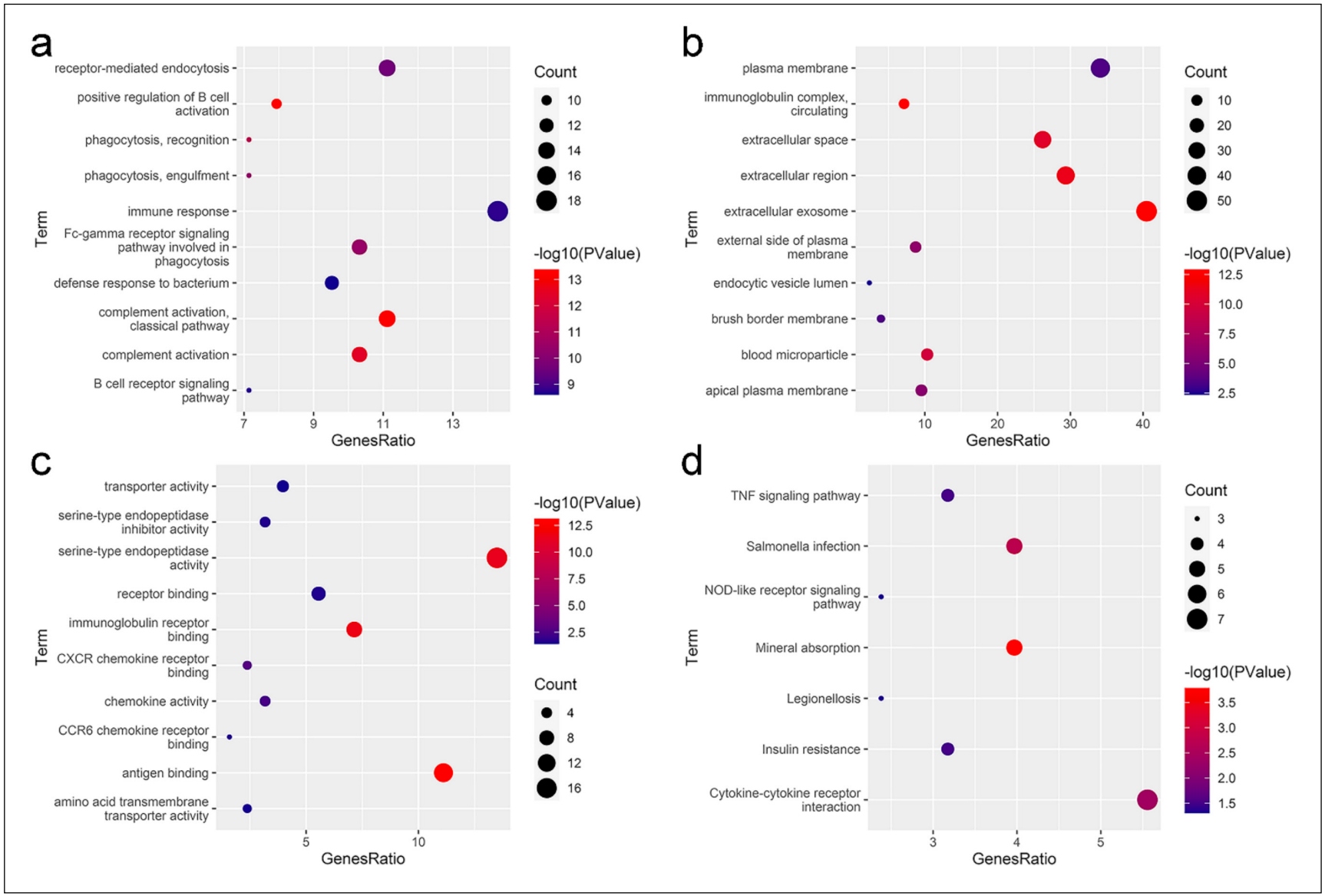

Figure 5. Enrichment analyses for the DEGs among the patients with different CIFI. **a**, Top 10 of Enrichment of different Biological Process. **b**, Top 10 of Enrichment of different Cellular Component. **c**, Top 10 of Enrichment of different Molecular Function. **d**, Top 10 of Enrichment of different signaling pathways.

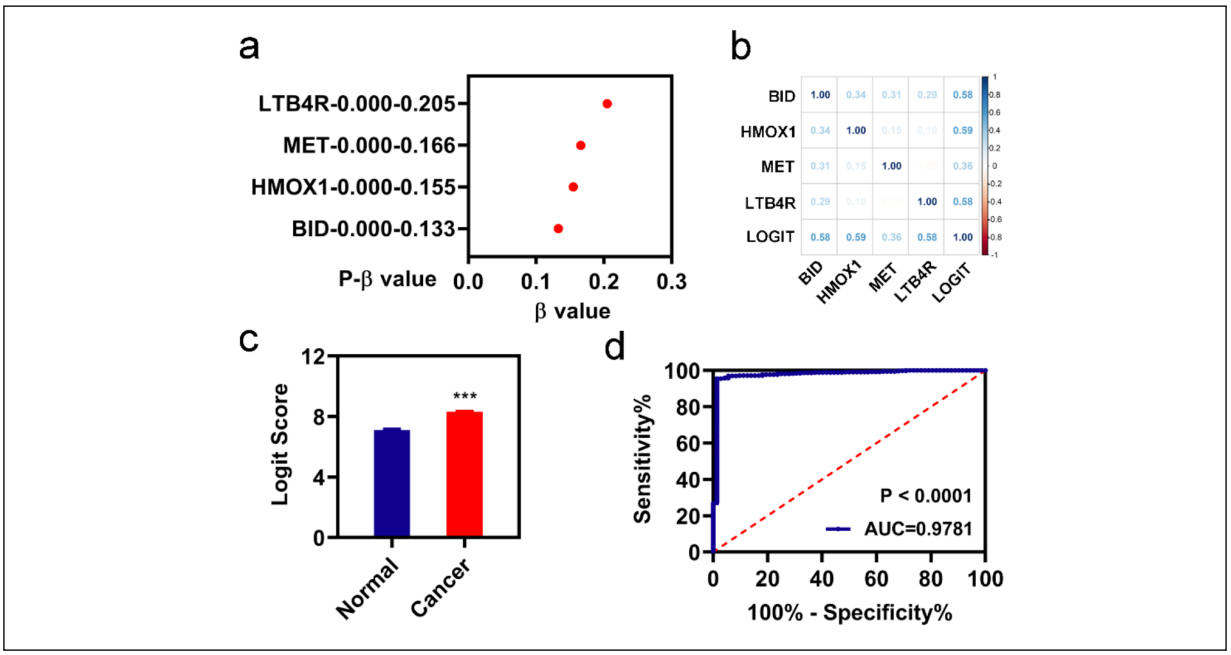

Figure 6. Construction of the diagnosis model. **a**, the β value of the four FI-DEGs analyzed by stepwise logistic regression. **b**, Correlation analysis of those 4 FI-DEGs with diagnosis values. **c**, Diagnosis values between normal and patients with KIRC. **d**, ROC curves of the diagnostic model. *** $p < 0.001$.

regulated DEGs). We performed GO and KEGG analyses for the 132 DEGs. The top 10 enriched GO and KEGG pathways are shown in Figure 5. Several immune-related GO and KEGG pathways were enriched, such as the positive regulation of B cell activation, immune response, and cytokine-cytokine receptor interaction (Figure 5a, 5d).

Construction and Validation of the Diagnosis Model

To understand whether these four candidate biomarkers could be used as diagnostic biomarkers for KIRC, we first performed a stepwise logistic regression analysis and constructed a diagnosis model (Figure 6a). The expression of these four FI-DEGs was markedly correlated with LOGIT expression (Figure 6b). The LOGIT score was considerably increased in patients with KIRC (Figure 6c). We then carried out validation analyses and found that the sensitivity and specificity of the diagnosis model were 0.9547 and 0.9861, respectively (Table I). The AUC value of the diagnostic model was 0.9781 (Figure 6d).

Discussion

KIRC is a malignant cancer originating from the renal epithelium, which accounts for approximately 75% of kidney cancer cases[2]. Previous studies[16] have demonstrated that 60% of patients with KIRC die within the first 2-3 years, and 30% of the patients with KIRC are always diagnosed with metastases. The prognosis of patients with metastatic KIRC is poor[17-19]; therefore, it is important to identify reliable biomarkers for the diagnosis and prognosis of KIRC.

In the current study, we first downloaded the corresponding data from 72 controls and 530 patients with KIRC from the TCGA database. We performed univariate Cox regression analyses, followed by LASSO analyses, for the 367 FI-DEGs and found that 19 FI-DEGs correlated with OS. We then performed multivariate Cox regression analyses for the 19 FI-DEGs and found that four FI-DEGs independently correlated with the OS of KIRC patients. We constructed a risk assessment model using these four FI-DEGs and evaluated their feasibility for predicting the prognosis of KIRC. These results indicate that the four FI-DEGs could be used as prognostic biomarkers for KIRC, as measured by the AUC evaluation. Additionally, we constructed a diagnostic model using the four FI-DEGs. The results indicate that these four FI-DEGs could also be used as diagnostic biomarkers for KIRC, as measured by their sensitivity and specificity. BID (BH3 Interacting Domain Death agonist) is a pro-apoptotic member

of the Bcl-2 family. Gryko et al[20] found that BID expression was positive in 53.6% of patients with gastric cancer. Al-Asmari et al[21] found that scorpion venom could attenuate the invasion of colorectal and breast cancer cell lines. Moreover, the anticancer effect of scorpion venom is associated with the downregulation of BID[21]. Orzechowska et al[22] found that BID could be a potential therapeutic target for cervical carcinoma and advanced prostate cancer. In the present study, we found that the expression of BID markedly increased and correlated with the OS of KIRC patients, reinforcing the relationship between BID and cancer. Activation of the MET tyrosine kinase receptor pathway is associated with the appearance of several hallmarks of cancer[23]. In renal cancer, Chen et al[24] found that the expression of MET increased in 8 of 10 KIRC tissue samples compared to that in the adjacent normal tissue. MET expression was independently associated with OS in KIRC. Macher-Goeppinger et al[25] found that high MET expression and MET copy number gains were associated with an aggressive phenotype and unfavorable patient outcomes. These results indicate that MET may be a prognostic biomarker for KIRC. In the current study, we found that KIRC expression was considerably increased in patients with KIRC and was correlated with the OS of KIRC. The present study reinforced the feasibility of MET as a prognostic biomarker for KIRC. LTB4R (Leukotriene B4 receptor) is a member of the GPCR family. In general, tumor tissues displayed higher levels of LTB4R expression than the normal tissues[26]. Ihara et al[27] found that suppression of the LTB4 signaling pathway could induce apoptosis and suppress cell proliferation in colon cancer. Tong et al[28] found that LTB4 increased the proliferation of pancreatic cancer cell lines. However, the LTB4R antagonist LY293111 caused both time- and concentration-dependent inhibition of the pancreatic cancer cell lines[28]. We found that the expression of LTB4R markedly increased in patients with KIRC, which is consistent with other cancers. Additionally, Wu et al[29] also found that LTB4R may be a novel immune-related prognostic biomarker for KIRC. The present study further confirmed the possibility of using LTB4R as a prognostic biomarker for KIRC[30]. HMOX1 (heme oxygenase-1) is a stress-induced enzyme that catalyzes the degradation of heme to carbon monoxide, iron, and biliverdin. HMOX1 is frequently upregulated in different types of tumors and correlates with tumor progression, aggressiveness, resistance to therapy, and poor prognosis[31]. Ren et al[32] found that downregulation of HMOX1 promoted apoptosis and inhibited proliferation and invasion of gastric cancer cell lines. Chang et al[33] found that HMOX1 is markedly related to the OS of patients with KIRC. In addition, Zhao et al[34] found that high expression of HMOX1 predicts poor prognosis in ovarian cancer patients and promotes proliferation and aggressiveness of ovarian cancer cells.

Table I. Sensitivity and specificity of the diagnosis model.

	Real Cancer	Real Normal
Predicted Cancer	506	1
Predicted Normal	24	71
Total	530	72
Correct	506	71
Sensitivity	0.9547	
Specificity		0.9861

Additionally, there have been several studies on ferroptosis- and immune-related genes as biomarkers of KIRC. Hong et al[35] found 12 molecular signatures that could be prognosis biomarkers[35]. The AUC value of the risk model based on the 12 signatures was > 0.7. Similarly, Wu et al[36] also found that six genes (TRAF6, FYN, IKBKG, LAT2, C2, IL4, EREG, TRAF2, and IL12A) could be prognostic factors for KIRC. This model had good sensitivity and specificity because the AUC value at five years was over 0.712. Although the AUC values in our present model were comparable to theirs, we used fewer prognostic biomarker genes. This situation increases the feasibility of the application of the proposed model.

Conclusions

Regulation of ferroptosis and immunity is a novel treatment option for patients with cancers that have been determined in recent years. In the present study, we constructed a diagnostic and prognostic model for KIRC using ferroptosis and immune-related genes as biomarkers. Our study not only contributes to our understanding of the roles of ferroptosis and immunity in development, but also contributes to the diagnosis and prognosis of KIRC, although it remains to be further studied whether these four biomarkers could actually be used in the clinic.

Conflict of Interest

The authors declare no conflict of interest.

Acknowledgements

Not applicable.

Funding

This project was financially supported by the Foundation of Hunan University of Medicine (2020122004, 20KJPY 02) and Changsha Medical College of The Training Object of Young Backbone Teachers in Colleges and Universities in Hunan Province.

Authors' Contributions

All the authors have read and approved the manuscript. Z.X. and Y.Z. conceived and designed the experiments; X.X. performed the analyses; Y.L., J.L., H.Z1., H.Z2., Q.Z., P.B., and T.D. helped analyze the data; X.X. wrote the paper. All the authors have read and approved the manuscript.

Data Availability

The data that support the findings of this study are openly available in TCGA at https://portal.gdc.cancer.gov/.

Reference

1) Sung H, Ferlay J, Siegel RL, Laversanne M, Soerjomataram I, Jemal A, Bray F. Global cancer statistics 2020: Globocan estimates of incidence and mortality worldwide for 36 cancers in 185 countries. CA Cancer J Clin 2021; 71: 209-249.
2) Hsieh JJ, Purdue MP, Signoretti S, Swanton C, Albiges L, Schmidinger M, Heng DY, Larkin J, Ficarra V. Renal cell carcinoma. Nat Rev Dis Primers 2017; 3: 17009.
3) Zhang Q, Shi J, Yuan F, Wang H, Fu W, Pan J, Huang Y, Yu J, Yang J, Chen Z. Higher expression of xpf is a critical factor in intrinsic chemotherapy resistance of human renal cell carcinoma. Int J Cancer 2016; 139: 2827-2837.
4) Cui H, Shan H, Miao MZ, Jiang Z, Meng Y, Chen R, Zhang L, Liu Y. Identification of the key genes and pathways involved in the tumorigenesis and prognosis of kidney renal clear cell carcinoma. Sci Rep 2020; 10: 4271.
5) Cairns P. Renal cell carcinoma. Cancer Biomark 2010; 9: 461-473.
6) Siska PJ, Beckermann KE, Rathmell WK, Haake SM. Strategies to overcome therapeutic resistance in renal cell carcinoma. Urol Oncol 2017; 35: 102-110.
7) Barata PC, Rini BI. Treatment of renal cell carcinoma: Current status and future directions. CA Cancer J Clin 2017; 67: 507-524.
8) Mejean A, Ravaud A, Thezenas S, Colas S, Beauval JB, Bensalah K, Geoffrois L, Thiery-Vuillemin A, Cormier L, Lang H, Guy L, Gravis G, Rolland F, Linassier C, Lechevallier E, Beisland C, Aitchison M, Oudard S, Patard JJ, Theodore C, Chevreau C, Laguerre B, Hubert J, Gross-Goupil M, Bernhard JC, Albiges L, Timsit MO, Lebret T, Escudier B. Sunitinib alone or after nephrectomy in metastatic renal-cell carcinoma. N Engl J Med 2018; 379: 417-427.
9) Wang D, Xie N, Gao W, Kang R, Tang D. The ferroptosis inducer erastin promotes proliferation and differentiation in human peripheral blood mononuclear cells. Biochem Biophys Res Commun 2018; 503: 1689-1695.
10) Wang W, Green M, Choi JE, Gijon M, Kennedy PD, Johnson JK, Liao P, Lang X, Kryczek I, Sell A, Xia H, Zhou J, Li G, Li J, Li W, Wei S, Vatan L, Zhang H, Szeliga W, Gu W, Liu R, Lawrence TS, Lamb C, Tanno Y, Cieslik M, Stone E, Georgiou G, Chan TA, Chinnaiyan A, Zou W. Cd8(+) t cells regulate tumour ferroptosis during cancer immunotherapy. Nature 2019; 569: 270-274.
11) Stockwell BR, Jiang X. A physiological function for ferroptosis in tumor suppression by the immune system. Cell Metab 2019; 30: 14-15.
12) Wang D, DuBois RN. Immunosuppression associated with chronic inflammation in the tumor microenvironment. Carcinogenesis 2015; 36: 1085-1093.
13) Li Z, Rong L. Cascade reaction-mediated efficient ferroptosis synergizes with immunomodulation for high-performance cancer therapy. Biomater Sci 2020; 8: 6272-6285.
14) Shi L, Liu Y, Li M, Luo Z. Emerging roles of ferroptosis in the tumor immune landscape: From danger signals to anti-tumor immunity. FEBS J 2022; 289: 3655-3665.
15) Liu Y, Zhang X, Zhang J, Tan J, Li J, Song Z. Development and validation of a combined ferroptosis and immune prognostic classifier for hepatocellular carcinoma. Front Cell Dev Biol. 2020; 8: 596679.
16) Mendoza-Alvarez A, Guillen-Guio B, Baez-Ortega A, Hernandez-Perez C, Lakhwani-Lakhwani S, Maeso MD, Lorenzo-Salazar JM, Morales M, Flores C. Whole-exome sequencing identifies somatic mutations associated with mortality in metastatic clear cell kidney carcinoma. Front Genet 2019; 10: 439.
17) Ljungberg B, Bensalah K, Canfield S, Dabestani S, Hofmann F, Hora M, Kuczyk MA, Lam T, Marconi L, Merseburger AS, Mulders P, Powles T, Staehler M, Volpe A, Bex A. Eau guidelines on renal cell carcinoma: 2014 update. Eur Urol 2015; 67: 913-924.
18) Forsea AM, Del Marmol V, de Vries E, Bailey EE, Geller AC. Melanoma incidence and mortality in europe: New estimates, persistent disparities. Br J Dermatol 2012; 167: 1124-1130.
19) Chaffer CL, Weinberg RA. A perspective on cancer cell metastasis. Science 2011; 331: 1559-1564.
20) Gryko M, Pryczynicz A, Zareba K, Kedra B, Kemona A, Guzinska-Ustymowicz K. The expression of bcl-2 and bid in gastric cancer cells. J Immunol Res 2014; 2014: 953203.
21) Al-Asmari AK, Riyasdeen A, Islam M. Scorpion venom causes upregulation of p53 and downregulation of bcl-xl and bid protein expression by modulating signaling proteins erk(1/2) and stat3, and DNA damage in breast and colorectal cancer cell lines. Integr Cancer Ther 2018; 17: 271-281.

22) Orzechowska EJ, Girstun A, Staron K, Trzcinska-Danielewicz J. Synergy of bid with doxorubicin in the killing of cancer cells. Oncol Rep 2015; 33: 2143-2150.
23) Moosavi F, Giovannetti E, Saso L, Firuzi O. Hgf/met pathway aberrations as diagnostic, prognostic, and predictive biomarkers in human cancers. Crit Rev Clin Lab Sci 2019; 56: 533-566.
24) Chen S, Zhu Y, Cui J, Wang Y, Xia Y, Song J, Cheng S, Zhou C, Zhang D, Zhang B, Shi B. The role of c-met in prognosis and clinicopathology of renal cell carcinoma: Results from a single-centre study and systematic review. Urol Oncol 2017; 35: 532.e15-532.e23.
25) Macher-Goeppinger S, Keith M, Endris V, Penzel R, Tagscherer KE, Pahernik S, Hohenfellner M, Gardner H, Grullich C, Schirmacher P, Roth W. Met expression and copy number status in clear-cell renal cell carcinoma: Prognostic value and potential predictive marker. Oncotarget 2017; 8: 1046-1057.
26) Long S, Ji S, Xiao K, Xue P, Zhu S. Prognostic and immunological value of ltb4r in pan-cancer. Math Biosci Eng 2021; 18: 9336-9356.
27) Ihara A, Wada K, Yoneda M, Fujisawa N, Takahashi H, Nakajima A. Blockade of leukotriene b4 signaling pathway induces apoptosis and suppresses cell proliferation in colon cancer. J Pharmacol Sci 2007; 103: 24-32.
28) Tong WG, Ding XZ, Hennig R, Witt RC, Standop J, Pour PM, Adrian TE. Leukotriene b4 receptor antagonist ly293111 inhibits proliferation and induces apoptosis in human pancreatic cancer cells. Clin Cancer Res 2002; 8: 3232-3242.
29) Wu HH, Yan X, Chen Z, Du GW, Bai XJ, Tuoheti K, Liu TZ. Gnrh1 and ltb4r might be novel immune-related prognostic biomarkers in clear cell renal cell carcinoma (ccrcc). Cancer Cell Int 2021; 21: 354.
30) Dunn LL, Kong SMY, Tumanov S, Chen W, Cantley J, Ayer A, Maghzal GJ, Midwinter RG, Chan KH, Ng MKC, Stocker R. Hmox1 (heme oxygenase-1) protects against ischemia-mediated injury via stabilization of hif-1alpha (hypoxia-inducible factor-1alpha). Arterioscler Thromb Vasc Biol 2021; 41: 317-330.
31) Furfaro AL, Traverso N, Domenicotti C, Piras S, Moretta L, Marinari UM, Pronzato MA, Nitti M. The nrf2/ho-1 axis in cancer cell growth and chemoresistance. Oxid Med Cell Longev 2016; 2016: 1958174.
32) Ren QG, Yang SL, Li PD, Xiong JR, Fang X, Hu JL, Wang QS, Chen RW, Chen YS, Wen L, Peng M. Low heme oxygenase-1 expression promotes gastric cancer cell apoptosis, inhibits proliferation and invasion, and correlates with increased overall survival in gastric cancer patients. Oncol Rep 2017; 38: 2852-2858.
33) Chang K, Yuan C, Liu X. Ferroptosis-related gene signature accurately predicts survival outcomes in patients with clear-cell renal cell carcinoma. Front Oncol 2021; 11: 649347.
34) Zhao Z, Xu Y, Lu J, Xue J, Liu P. High expression of ho-1 predicts poor prognosis of ovarian cancer patients and promotes proliferation and aggressiveness of ovarian cancer cells. Clin Transl Oncol 2018; 20: 491-499.
35) Hong Y, Lin M, Ou D, Huang Z, Shen P. A novel ferroptosis-related 12-gene signature predicts clinical prognosis and reveals immune relevancy in clear cell renal cell carcinoma. BMC Cancer 2021; 21: 831.
36) Wu G, Xu Y, Han C, Wang Z, Li J, Wang Q, Che X. Identification of a prognostic risk signature of kidney renal clear cell carcinoma based on regulating the immune response pathway exploration. J Oncol 2020; 2020: 6657013.